DOI 10.5162/SMSI2023/E5.2

Integration of a High-Precision 3D Sensor into a 3D Thermography System

Miguel Méndez[1], Sebastian Schramm[1], Robert Schmoll[1], Andreas Kroll[1]
[1] University of Kassel, Department of Measurement and Control
Mönchebergstraße 7, 34109 Kassel, Germany
miguel.mendez@mrt.uni-kassel.de

Summary:
In this paper, the integration of an industrial high-precision 3D sensor into a 3D Thermography System is presented. A large size object was recorded using the previous and the new system. The obtained point cloud geometry was evaluated by means of a non-referenced point cloud quality assessment approach. The implementation showed an improvement of the local curvature and anisotropy.

Keywords: 3D Thermography, Sensor Data Fusion, No-Reference Point Cloud Quality Assessment.

Introduction

The capability of energy loss detection and quantification is one of the most relevant industrial sustainability challenges. The development of fast response and reliable thermal inspection methodologies is gaining importance, addressing topics such as infrared thermography and sensor data fusion. A 3D Thermography System (3DTS) enables the creation of a live 3D model, which eases the interpretation and analysis of results, compared with 2D thermal images.

A 3DTS was developed by [1] and compared with the obtained system by [2], where the capability of the concept for measuring large size objects was extended. For both cases, an infrared camera was used in conjunction with a relative low-cost depth and RGB sensor. In this work, the improvement of the reconstructed model geometry by the implementation of an industrial high-precision 3D sensor (MotionCam-3D (MC3D) by Photoneo) for the depth measurement task is presented.

3D Thermography System

The improved system consists of a long-wave infrared (LWIR) camera, a structured light sensor MC3D and a RGB camera (see Fig. 1). The processing tasks are performed by a developed C++ (CUDA) executable. It exploits the hardware capabilities of a high-end graphics card laptop (GeForce GTX 980M, 4 GB VRAM) by implementing multithreading computations. These computations range from the unification of the three camera coordinate systems to the point cloud fusion, by means of an extended processing algorithm from [3], as described in [2].

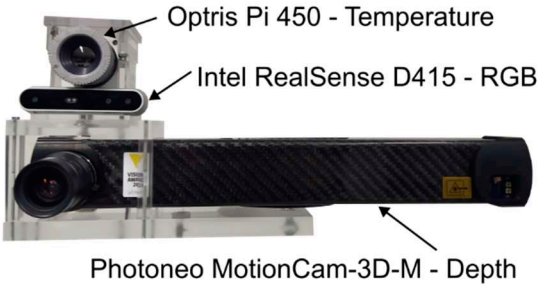

Fig. 1: Assembled 3D Thermography System.

Two main problems had to be solved for the integration of the MC3D. The first one was the perturbation of the RGB model texture caused by the red-light pattern of the MC3D, which was solved by the suppression of the red component from the color vector. The second one was the temporal synchronization of the three sensor frames. As the post-processing features of the MC3D introduce a time delay of the depth frames, the system must search backwards in the temperature and color buffers for the respective frames, which match the last depth measurement in time. When the three images are temporally quasi-aligned, they are processed by the extended Elastic Fusion algorithm.

3DTS evaluation

A flow measurement test bench (see Fig. 2) was investigated using the previous and the new 3DTS. The obtained point cloud (PC) was assessed following the approach suggested by [4], since it is not dependent on a reference point cloud. Each point was grouped in a neighborhood with the 9 closest points (10 members), using the Euclidean distance metric.

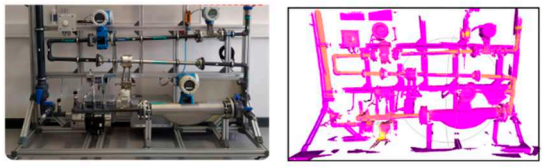

Fig. 2: Flow measurement test bench (left) and an example of the 3D Thermogram (right).

For each point, the surface variation could be approximated to the covariance matrix C_i [5]:

$$C_i = \frac{1}{10}\sum_{j=1}^{10}(p_j - \hat{p})(p_j - \hat{p})^T \quad (1)$$

Where p_j and $\hat{p}$ are cartesian coordinate vectors and represent the j-th member and the centroid of the neighborhood, respectively. Formulating the eigenvector problem:

$$C_i \cdot v_l = \lambda_l \cdot v_l, l \in \{1,2,3\} \quad (2)$$

With the eigenvectors (v_1, v_2, v_3) and the corresponding eigenvalues ($\lambda_1 > \lambda_2 > \lambda_3$), the variation of the p_i along the direction of v_l are represented by λ_l [6]. The curvature:

$$Cur(p_i) = \frac{\lambda_3}{\lambda_1+\lambda_2+\lambda_3} \quad (3)$$

and the anisotropy:

$$A(p_i) = \frac{\lambda_1-\lambda_3}{\lambda_1} \quad (4)$$

formulations were chosen, since they represent the local roughness and the geometrical variation, respectively. These metrics are important for the thermographic data fusion due to the emissivity dependency with the surface normal angle [1].

Results and discussion

One exemplary detail of the obtained PCs is presented in Fig. 3. A visual improvement on the geometry quality is observed with the MC3D. The system extension provides for straighter lines and flatter surfaces, in addition to a diminution of the number of aleatory points around the recorded objects. This is visible in the proposed indicators (see Fig. 4), where the local curvature is reduced, and the neighborhoods are more aligned in a single direction, as the anisotropy indicates. Less dispersion is also remarkable with the MC3D, indicating an overall impact for the complete geometry.

Conclusions

An industrial MC3D was integrated into a 3DTS. The quality of the new model was compared to respective one of the previous system. The results showed a significant improvement of the analyzed local curvature and anisotropy.

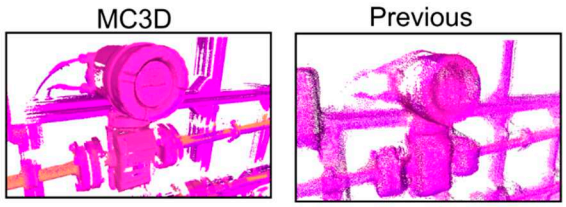

Fig. 3: Detail of the PCs obtained with both systems.

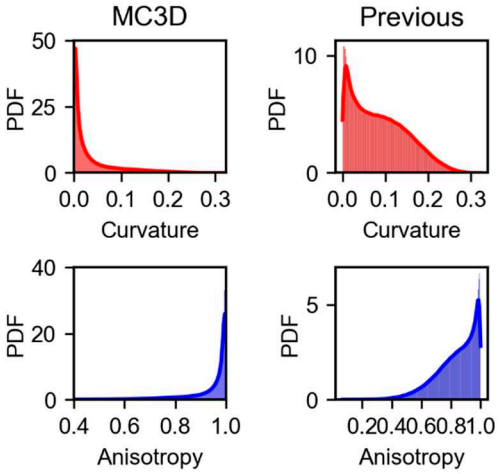

Fig. 4: Obtained normalized Probability Density Function (PDF) for the curvature and the anisotropy features.

References

[1] A. Ordonez Muller and A. Kroll, "Generating High Fidelity 3-D Thermograms with a Handheld Real-Time Thermal Imaging System," *IEEE Sens J*, vol. 17, no. 3, pp. 774–783, Feb. 2017, doi: 10.1109/JSEN.2016.2621166.

[2] S. Schramm, P. Osterhold, R. Schmoll, and A. Kroll, "Generation of Large-Scale 3D Thermograms in Real-Time Using Depth and Infrared Cameras," *15th Quantitative Infrared Thermography*, Dec. 2020. doi: 10.21611/qirt.2020.008.

[3] T. Whelan, S. Leutenegger, R. F. Salas-Moreno, B. Glocker, and A. J. Davison, "ElasticFusion: Dense SLAM Without A Pose Graph." *Robotics: Science and Systems*, 2015, doi:10.15607/RSS.2015.XI.001.

[4] Z. Zhang, W. Sun, X. Min, T. Wang, W. Lu, and G. Zhai, "No-Reference Quality Assessment for 3D Colored Point Cloud and Mesh Models," *IEEE Transactions on Circuits and Systems for Video Technology*, 2022, doi: 10.1109/TCSVT.2022.3186894.

[5] R. Rusu, "Semantic 3D Object Maps for Everyday Manipulation in Human Living Environments," *KI-Künst Intell* 24, 345 -348 (2010), doi: 10.1007/s13218-010-0059-6

[6] M. Pauly, M. Gross, L. P. Kobbelt, E. Zürich, and R. Aachen, "Efficient Simplification of Point-Sampled Surface." *Proceedings of the IEEE Visualization Conference*. 1. 163 – 170, doi: 10.1109/VISUAL.2002.1183771.